

The bottleneck and ceiling effects in quantized tracking control of heterogeneous multi-agent systems under DoS attacks

Shuai Feng^a, Maopeng Ran^b, Baoyong Zhang^a, Lihua Xie^c, Shengyuan Xu^{* a}

^a*School of Automation, Nanjing University of Science and Technology, Nanjing 210094, China*

^b*School of Automation Science and Electrical Engineering, Beihang University, Beijing 100191, China and the Zhongguancun Laboratory, Beijing 100094, China*

^c*School of Electrical and Electronics Engineering, Nanyang Technological University, Singapore 68000, Singapore*

Abstract

In this paper, we investigate tracking control of heterogeneous multi-agent systems under Denial-of-Service (DoS) attacks and state quantization. Dynamic quantized mechanisms are designed for inter-follower communication and leader-follower communication. Zooming-in and out factors, and data rates of both mechanisms for preventing quantizer saturation are provided. Our results show that by tuning the inter-follower quantized controller, one cannot improve the resilience beyond a level determined by the data rate of leader-follower quantized communication, i.e., the ceiling effect. Otherwise, overflow of followers' state quantizer can occur. On the other hand, if one selects a "large" data rate for leader-follower quantized communication, then the inter-follower quantized communication determines the resilience, and further increasing the data rate for leader-follower quantized communication cannot improve the resilience, i.e., the bottleneck effect. Simulation examples are provided to justify the results of our paper.

1 Introduction

Control of multi-agent systems has attracted substantial attention of researchers. An agent refers to a subsystem in a large-scale system consisting of multiple agents and can be a different subject depending on the context. For example, an agent is a drone in a UAV swarm or a car in a vehicle platoon [1]. Agents are spatially distributed and hence the realization of control significantly depends on the quality of information exchanged among the agents via wireless communication networks. However, the challenges of malicious cyber attacks on information also emerge [2].

The control problems under packet losses have been well studied, e.g. in [3] for stochastic packet losses, and the case of DoS attacks inducing malicious packet losses has been studied in [4–6]. This paper deals with DoS attacks. The communication failures induced by DoS can exhibit a temporal profile quite different from those caused by genuine packet losses due to network congestion; particularly packet dropouts resulting from malicious DoS need not follow a given class of probability distributions [7], and therefore the analysis techniques relying on probabilistic arguments may not be applicable.

Attention has been focused on centralized systems under DoS attacks for achieving stability [8, 9], attack detection and control [10] and state estimation [11]. In [12], the authors study a stabilization problem under energy-constrained PWM DoS signals, and propose time and event triggering

strategies under partially known and unknown attack information, respectively. The paper [13] describes DoS attacks by a Markov modulated model, in which the control packets are jammed stochastically. In [14], the authors model the interplay between a DoS attacker and a defender as a two-player zero-sum game and compute the saddle-point equilibrium. Recently, multi-agent systems under DoS attacks have been increasingly investigated, e.g., consensus, state estimation and real-time attack detection [15–17]. In [18], the authors propose a novel data-driven based algorithm to estimate the unknown switching matrices of the exosystems, and realize output regulation under DoS for heterogeneous multi-agent systems.

For multi-agent systems, the amount of data can be large especially when the number of agents is large. Consequently, agents can be subject to bandwidth limitation, and hence signals are subject to coarse quantization [19–24]. Dynamic quantization for centralized systems in the presence of DoS attacks has been recently studied in [8, 25], in which the quantization mechanisms have zooming-out and in capabilities for mitigating the influence of DoS-induced packet losses and achieving asymptotic stability, respectively. Dynamic quantization has also been established for consensus of multi-agent systems without packet losses [26], in which only the zooming-in capability is developed. Recently, the papers [27–29] study consensus problems under DoS attacks and dynamic quantization. In [27, 28], quantization mechanisms with zooming-in and out capabilities are developed for homogeneous agents. An approach for designing a tight zooming-out parameter is provided, but the condition for consensus is subject to an additional constraint of DoS frequency [28]. As will be shown later, the approach in our paper is free from the additional DoS-frequency constraint.

Email addresses: s.feng@njust.edu.cn (Shuai Feng), ranmp@buaa.edu.cn (Maopeng Ran), baoyongzhang@njust.edu.cn (Baoyong Zhang), ELHXIE@ntu.edu.sg (Lihua Xie), syxu@njust.edu.cn (Shengyuan Xu*).

In practice, a variety of agents may need to cooperate to complete a complicated task, i.e., cooperation of heterogeneous multi-agent systems [30, 31]. Consequently, those results for the control of homogeneous agents may not hold. In [29], heterogeneous nonlinear multi-agent systems under DoS and quantization were studied, while the focus is on the common consensus problem instead of tracking control. In this paper, we are interested in output tracking control of heterogeneous multi-agent systems under quantized communication and DoS attacks, in which the quantizer has a finite quantization range. The quantized controllers to be designed should prevent quantizer saturation all the time. Unlike DoS-free scenarios, the tracking errors can diverge under DoS attacks, and consequently some measurements can overflow the range of the quantizer if the quantized controllers for DoS-free scenarios are implemented.

For quantized tracking control of multi-agent systems, one can classify the overall information flow into the part for leader-follower quantized communication and the part for inter-follower quantized communication. In [27, 32], the leader-follower communication and inter-follower communication adopt an identical quantization mechanism. However, this may not provide optimal performance in communication resource allocation and control. One may also lose the insights about the interactions between the leader-follower and inter-follower quantized communication. For example, in order to save communication resource, one can select a data rate for the leader-follower quantized communication as close as possible to the minimum data rate [33], under which the followers can still estimate the leader's state asymptotically. As will be shown in this paper, such a data rate (of the leader-follower quantized communication) can influence the inter-follower quantized communication, i.e., the quantizer for quantizing followers' state can have overflow problem. In this paper, resilience refers to a bound characterizing the amount of DoS attacks under which multi-agent systems can achieve quantized tracking control. Under DoS attacks, it is interesting and also important to know whether the leader-follower quantized communication or the inter-follower quantized communication influences more on the resilience. From a practical viewpoint, this can actually lead us to the optimal strategies of limited bandwidth allocation for real applications.

The paper's contributions are twofold: a) design heterogeneous dynamic quantized controllers for the tracking control of heterogeneous multi-agent systems, b) discover the interactions between the leader-follower quantized communication and inter-follower quantized communication, and the consequent influences on the resilience of tracking control against DoS attacks. We reveal that the leader-follower quantized communication can cause ceiling effect and the inter-follower communication can cause bottleneck effect. Specifically, for a given communication topology and a number of bits for the quantization of the leader's state, by tuning the followers' quantized controller, one cannot improve the resilience beyond a level determined by the data rate of leader-follower quantized communication, i.e., the ceiling effect. Otherwise, overflow problems for quantizing follow-

ers' state can occur. For the bottleneck effect, if one selects a "large" data rate for leader-follower quantized communication, further enlarging it cannot improve the resilience. Then the inter-follower quantized communication is the bottleneck of the resilience, which depends on the choices of the zooming-in and out factors for followers' state quantization. We emphasize that, by our quantized controller design, the tightness for zooming-in factor is the same for DoS-free case [26], and the zooming-out factor is tight, i.e., arbitrarily approaching the spectral radius of the leader's dynamic matrix.

This paper is organized as follows. In Section 2, we introduce the framework consisting of the control objectives, the heterogeneous leader and followers, and the class of DoS attacks. Section 3 presents the design of quantized controllers. The results of the paper are presented in Section 4. Numerical examples are presented in Section 5, and finally Section 6 ends the paper with conclusions and future research.

Notation. We denote by \mathbb{R} the set of reals. Given $b \in \mathbb{R}$, $\mathbb{R}_{\geq b}$ and $\mathbb{R}_{> b}$ denote the sets of reals no smaller than b and reals greater than b , respectively; $\mathbb{R}_{\leq b}$ and $\mathbb{R}_{< b}$ represent the sets of reals no larger than b and reals smaller than b , respectively; \mathbb{Z} denotes the set of integers. For any $c \in \mathbb{Z}$, we denote $\mathbb{Z}_{\geq c} := \{c, c+1, \dots\}$. Let $\lfloor v \rfloor$ be the floor function such that $\lfloor v \rfloor = \max\{o \in \mathbb{Z} | o \leq v\}$. Given a vector y and a matrix Γ , let $\|y\|$ and $\|y\|_{\infty}$ denote the 2- and ∞ - norms of vector y , respectively, and $\|\Gamma\|$ and $\|\Gamma\|_{\infty}$ represent the corresponding induced norms of matrix Γ . Let $\rho(\Gamma)$ denote the spectral radius of Γ . Given an interval \mathcal{I} , $|\mathcal{I}|$ denotes its length. The Kronecker product is denoted by \otimes . We let " $\dot{\cdot}$ " represent element-wise division of vectors, e.g., $\frac{[x_1 \ x_2]^T}{[y_1 \ y_2]^T} = [x_1/y_1 \ x_2/y_2]^T$. Let " \circ " denote the element-wise multiplication of two vectors, e.g., $[a_1 \ a_2]^T \circ [b_1 \ b_2]^T = [a_1 b_1 \ a_2 b_2]^T$. In our paper, a switched system refers to a class of systems in the form: $x(k+1) = A_i x(k)$, $i \in \{1, 2, \dots, c\}$, in which the value of i depends on the switching rules.

2 Framework

Communication graph: We let graph $\mathcal{G} = (\mathcal{N}, \mathcal{E})$ denote the communication topology among the followers, where $\mathcal{N} = \{1, 2, \dots, N\}$ denotes the set of follower agents and $\mathcal{E} \subseteq \mathcal{N} \times \mathcal{N}$ denotes the set of edges. Let \mathcal{N}_i denote the set of the neighbors of agent i , where $i = 1, 2, \dots, N$. We assume that the graph \mathcal{G} is undirected and connected. Let $\mathcal{A}_{\mathcal{G}} = [a_{ij}] \in \mathbb{R}^{N \times N}$ denote the adjacency matrix of \mathcal{G} , where $a_{ij} > 0$ if and only if $j \in \mathcal{N}_i$ and $a_{ii} = 0$. Define the Laplacian matrix $\mathcal{L}_{\mathcal{G}} = [l_{ij}] \in \mathbb{R}^{N \times N}$, in which $l_{ii} = \sum_{j=1}^N a_{ij}$ and $l_{ij} = -a_{ij}$ if $i \neq j$. For the leader-follower communication, we assume that only a fraction of the followers can receive information from the leader. Let a_{i0} represent the leader-follower interaction, i.e., if follower i can directly receive the information from the leader, then $a_{i0} > 0$, and otherwise $a_{i0} = 0$. Moreover, we let the diagonal matrix be $\mathcal{D} = \text{diag}(a_{10}, a_{20}, \dots, a_{N0}) \in \mathbb{R}^{N \times N}$. Let $\tilde{\lambda}_i$ ($i = 1, 2, \dots, N$) denote the eigenvalues of $\mathcal{L}_{\mathcal{G}} + \mathcal{D}$.

System description: The follower agents interacting over the network \mathcal{G} are expressed as heterogeneous systems:

$$x_i(k+1) = A_i x_i(k) + B_i u_i(k) \quad (1a)$$

$$y_i(k) = C_i x_i(k) \quad (1b)$$

where $i \in \mathcal{N}$, $x_i(k) \in \mathbb{R}^{n_i}$ denotes the state of agent i , $u_i(k) \in \mathbb{R}^{w_i}$ denotes its control input, $y_i(k) \in \mathbb{R}^v$ denotes its output, and $A_i \in \mathbb{R}^{n_i \times n_i}$, $B_i \in \mathbb{R}^{n_i \times w_i}$ and $C_i \in \mathbb{R}^{v \times n_i}$. The sampling time between k and $k+1$ is Δ . We assume that (A_i, B_i) is stabilizable and thus there exists a feedback gain $K_i \in \mathbb{R}^{w_i \times n_i}$ such that $\rho(A_i + B_i K_i) < 1$. We assume that an upper bound of the initial condition $x_i(0)$ is known, i.e., $\|x_i(0)\|_\infty \leq C_{x_0} \in \mathbb{R}_{>0}$ ($i \in \mathcal{N}$). Note that C_{x_0} can be arbitrarily large as long as it satisfies this bound. This is for preventing the overflow of state quantization for the initial condition. The dynamics of the leader can be described by

$$v(k+1) = S v(k) \quad (2)$$

where $v(k) \in \mathbb{R}^{n_v}$ is the state and $S \in \mathbb{R}^{n_v \times n_v}$. We assume that $\rho(S) \geq 1$. Otherwise, as $v(k) \rightarrow 0$ when $k \rightarrow \infty$, one can simply realize the tracking control by locally stabilizing (1) under which $y_i(k) \rightarrow 0$. Similarly, we assume that an upper bound of the initial condition $v(0)$ is known, i.e., $\|v(0)\|_\infty \leq C_{v_0} \in \mathbb{R}_{>0}$.

We assume that $x_i(k)$ is available to the local controller of agent i . We also assume that only some of the followers can receive information from the leader. Followers can exchange information with their neighbor followers. We assume that transmissions are acknowledgment based and free of delay. Note that in a quantized control problem without packet losses, acknowledgments are not necessary [33, 34]. When packet losses and quantization coexist, acknowledgments are needed to ensure the synchronization of the signals in the encoders and decoders [3, 35]. Due to the data rate limitation, all the information exchanged via communication is encoded by limited numbers of bits. This implies that the transmitted signals are subject to quantization effect. In this paper, we develop two quantization mechanisms: one for followers' state quantization, and another for leader's state quantization. The motivations of adopting heterogeneous quantizers will be presented later (see Remark 3).

Quantizer for followers' state: Let $\chi \in \mathbb{R}$ be a scalar before quantization and $q_{R_f}(\cdot)$ be the quantization function for scalar input values as

$$q_{R_f}(\chi) = \begin{cases} 0 & -\sigma < \chi < \sigma \\ 2\psi\sigma & (2\psi-1)\sigma \leq \chi < (2\psi+1)\sigma \\ 2R_f\sigma & \chi \geq (2R_f+1)\sigma \\ -q_{R_f}(-\chi) & \chi \leq -\sigma \end{cases} \quad (3)$$

where $R_f \in \mathbb{Z}_{>0}$ is to be designed and $\psi = 1, 2, \dots, R_f$, and $\sigma \in \mathbb{R}_{>0}$. If the quantizer is unsaturated such that $|\chi| \leq (2R_f+1)\sigma$, then the quantization error satisfies $|\chi - q_{R_f}(\chi)| \leq \sigma$.

Quantizer for leader's state: Let $\pi_l := e_l/\omega_l$ be the l -th signal in a vector before quantization and $q_{\mathcal{R}_l}(\pi_l)$ represents the quantized signal of π_l encoded by \mathcal{R}_l bits, where $l =$

$1, 2, \dots, v$. The choices of $\mathcal{R}_l, e_l \in \mathbb{R}$ and $\omega_l \in \mathbb{R}_{>0}$ will be specified later. We implement a uniform quantizer such that

$$q_{\mathcal{R}_l}(\pi_l) := \begin{cases} \frac{\lfloor 2^{\mathcal{R}_l-1} \pi_l \rfloor + 0.5}{2^{\mathcal{R}_l-1}}, & \text{if } -1 \leq \pi_l < 1 \\ 1 - \frac{0.5}{2^{\mathcal{R}_l-1}}, & \text{if } \pi_l = 1 \end{cases} \quad (4)$$

if $\mathcal{R}_l \in \mathbb{Z}_{\geq 1}$, and $q_{\mathcal{R}_l}(\pi_l) = 0$ if $\mathcal{R}_l = 0$. Note that for any $\omega_l \in \mathbb{R}_{>0}$ the following holds:

$$|e_l - \omega_l q_{\mathcal{R}_l}(e_l/\omega_l)| \leq \omega_l/2^{\mathcal{R}_l}, \quad \text{if } |e_l|/\omega_l \leq 1 \quad (5)$$

for both cases [3].

2.1 Time-constrained DoS

We refer to DoS as the event under which all the encoded signals cannot be received by the decoders and it affects all the communication links simultaneously. We consider a general DoS model that describes the attacker's action by the frequency of DoS attacks and their duration. Let $\{h_q\}_{q \in \mathbb{Z}_{\geq 0}}$ with $h_0 \geq \Delta$ denote the sequence of DoS *off/on* transitions, that is, the time instants at which DoS exhibits a transition from zero (transmissions are possible) to one (transmissions are impossible). Hence, $H_q := \{h_q\} \cup [h_q, h_q + \tau_q]$ represents the q -th DoS time-interval, of a length $\tau_q \in \mathbb{R}_{\geq 0}$, over which the network is in DoS status. If $\tau_q = 0$, then H_q takes the form of a single pulse at h_q . Given $\tau, t \in \mathbb{R}_{\geq 0}$ with $t \geq \tau$, let $n(\tau, t)$ denote the number of DoS *off/on* transitions over $[\tau, t]$, and let $\Xi(\tau, t) := \bigcup_{q \in \mathbb{Z}_{\geq 0}} H_q \cap [\tau, t]$ be the subset of $[\tau, t]$ where the network is in DoS status.

Assumption 1 [4] (*DoS frequency*). There exist constants $\eta \in \mathbb{R}_{\geq 0}$ and $\tau_D \in \mathbb{R}_{>0}$ such that $n(\tau, t) \leq \eta + \frac{t-\tau}{\tau_D}$ for all $\tau, t \in \mathbb{R}_{\geq \Delta}$ with $t \geq \tau$. ■

Assumption 2 [4] (*DoS duration*). There exist constants $\kappa \in \mathbb{R}_{\geq 0}$ and $T \in \mathbb{R}_{>1}$ such that $|\Xi(\tau, t)| \leq \kappa + \frac{t-\tau}{T}$ for all $\tau, t \in \mathbb{R}_{\geq \Delta}$ with $t \geq \tau$. ■

Remark 1 In Assumption 1, τ_D can be considered as the average dwell-time between consecutive DoS *off/on* transitions, while η is the chattering bound. Assumption 2 expresses a similar requirement with respect to the duration of DoS. It expresses the property that, on the average, the total duration over which communication is interrupted does not exceed a certain *fraction* of time, as specified by $1/T$. The constant κ plays the role of a regularization term. It is needed because during a DoS interval, one has $|\Xi(h_q, h_q + \tau_q)| = \tau_q > \tau_q/T$. Thus κ serves to make Assumption 2 consistent. Conditions $\tau_D > 0$ and $T > 1$ imply that DoS cannot occur at an infinitely fast rate or be always active. ■

Control objectives: We seek to design a distributed controller $u_i(k)$ such that the quantizers in (3) and (4) do not saturate under DoS attacks; the outputs of the followers can track the state of the leader: $\lim_{k \rightarrow \infty} y_i(k) = v(k)$.

3 Controller design

The following lemma is necessary to relax the constraints of dwell time of switched systems and obtain a tight data rate (see Remarks 2 and 3).

Lemma 1 [33] There exist (bounded) matrices $E(k) \in \mathbb{R}^{n_v \times n_v}$ and $T \in \mathbb{R}^{n_v \times n_v}$, and a transformation $\bar{v}(k) =$

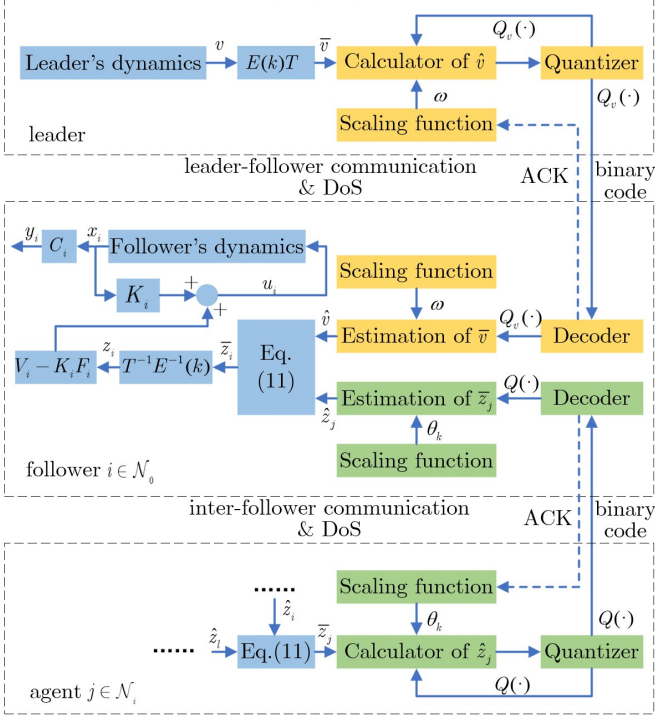


Fig. 1. Control structure over the network. Agent $i \in \mathcal{N}_0$ is a direct follower of the leader. Agent $j \in \mathcal{N}_i$ is a neighbor of agent i . l is the index for agent $l \in \mathcal{N}_j$. ACK denotes acknowledgments.

$E(k)Tv(k)$, possibly time-varying, transforming (2) into $\bar{v}(k+1) = \bar{S}\bar{v}(k)$, $\bar{S} = \text{diag}(\bar{S}_1, \dots, \bar{S}_p) \in \mathbb{R}^{n_v \times n_v}$ (6) where $p \in \mathbb{Z}_{\geq 1}$ denotes the number of sub-matrices in \bar{S} . Let $r = 1, 2, \dots, p$, then one has

$$\bar{S}_r = \begin{bmatrix} \lambda_r & 1 & & \\ & \lambda_r & 1 & \\ & & \ddots & \ddots \\ & & & \lambda_r \end{bmatrix} \in \mathbb{R}^{n_r \times n_r} \quad (7)$$

corresponding to the real eigenvalue $\lambda_r \in \mathbb{R}$ of S , and

$$\bar{S}_r = \begin{bmatrix} \zeta_r I_2 & r^{-1}(\phi) & & \\ & \zeta_r I_2 & r^{-1}(\phi) & \\ & & \ddots & \ddots \\ & & & r^{-1}(\phi) \\ & & & & \zeta_r I_2 \end{bmatrix} \in \mathbb{R}^{2n_r \times 2n_r} \quad (8)$$

corresponding to the complex eigenvalues $\lambda_r = \zeta_r(\cos \phi \pm i \sin \phi)$ with $\zeta_r \geq 0$ and

$$r(\phi) = \begin{bmatrix} \cos \phi & \sin \phi \\ -\sin \phi & \cos \phi \end{bmatrix}, \quad I_2 = \begin{bmatrix} 1 & 0 \\ 0 & 1 \end{bmatrix}. \quad \blacksquare$$

If S has only real eigenvalues, the time-varying part in the transformation $\bar{v}(k) = E(k)Tv(k)$ is not needed, i.e., $\bar{v}(k) = Tv(k)$. Then, one only has the Jordan blocks in (7).

Assumption 3 For $i \in \mathcal{N}$, we assume that there exists (F_i, V_i) satisfying $F_i S = A_i F_i + B_i V_i$ and $I_v = C_i F_i$,

where I_v is the identity matrix of dimension $n_v \times n_v$, and $V_i \in \mathbb{R}^{w_i \times n_v}$ and $F_i \in \mathbb{R}^{n_i \times n_v}$. \blacksquare

Assumption 3 is a typical assumption for cooperative control of heterogeneous multi-agent systems [30]. We refer the readers to [36] for more details.

Controller design: As shown in Figure 1, for follower agent $i \in \mathcal{N}$, we propose the local control input

$$u_i(k) = K_i x_i(k) + (V_i - K_i F_i) z_i(k) \quad (9)$$

in which

$$z_i(k) := T^{-1} E^{-1}(k) \bar{z}_i(k) \in \mathbb{R}^{n_v}. \quad (10)$$

The dynamics of $\bar{z}_i(k)$ in (10) follows

$$\bar{z}_i(k+1) = \begin{cases} \bar{S} \bar{z}_i(k) + \bar{K} \sum_{j=1}^N a_{ij} (\hat{z}_j(k) - \hat{z}_i(k)) \\ \quad + \bar{K} a_{i0} (\hat{v}(k) - \hat{z}_i(k)), & \text{if } k \notin H_q \\ \bar{S} \bar{z}_i(k), & \text{if } k \in H_q \end{cases} \quad (11)$$

where $\hat{z}_j(k) \in \mathbb{R}^{n_v}$ and $\hat{v}(k) \in \mathbb{R}^{n_v}$ are the estimates of $\bar{z}_j(k)$ and $\bar{v}(k)$, respectively, and $\bar{K} \in \mathbb{R}^{n_v \times n_v}$ is a design parameter to be given later. The computation of $\hat{z}_j(k)$ in (11) follows

$$\hat{z}_j(k) = \begin{cases} \bar{S} \hat{z}_j(k-1) + \theta_{k-1} Q \left(\frac{\bar{z}_j(k) - \bar{S} \hat{z}_j(k-1)}{\theta_{k-1}} \right) & \text{if } k \notin H_q \\ \bar{S} \hat{z}_j(k-1) & \text{if } k \in H_q \end{cases} \quad (12)$$

where $j \in \{i\} \cup \mathcal{N}_i$ and $Q(\cdot) = [q_{R_f}(\cdot) \cdots q_{R_f}(\cdot)]^T$ is the vector version of (3). The scaling parameter θ_k updates as

$$\theta_k = \begin{cases} \gamma_1 \theta_{k-1}, & \text{if } k \notin H_q \\ \gamma_2 \theta_{k-1}, & \text{if } k \in H_q \end{cases} \quad (13)$$

where $\gamma_1 < 1$ and $\gamma_2 > 1$ are zooming in and out parameters, respectively. We assume that the algorithms in (12) and (13) are embedded in the encoders and decoders of $i \in \mathcal{N}$ with identical initial conditions. Under DoS attacks, the variables in $Q(\cdot)$ may diverge. Therefore, the quantizers must zoom out by using γ_2 and increase their ranges so that the states can be measured properly. If the transmissions succeed, the quantizers zoom in and $\theta_k \in \mathbb{R}_{>0}$ decreases by using γ_1 . By adjusting the scaling parameter θ_k in $Q(\cdot)$ dynamically, the state will be kept within the limited quantization range without saturation and can converge asymptotically. The ranges of γ_1 and γ_2 , and θ_0 will be specified later. Note that γ_1, γ_2 and θ_0 in our paper are homogeneous among the followers. It is interesting to design distributed scaling parameters, e.g., γ_1^i and γ_2^i . In this situation, the new scaling parameter θ_k in (13) will be a vector, and zooming-in and out factors composed by γ_1^i and γ_2^i will be matrices. This case will be left for future research.

The update of $\hat{v}(k)$ in (11) is given by

$$\hat{v}(k) = \begin{cases} \bar{S}(\hat{v}(k-1) - \omega(k-1) \circ Q_v \left(\frac{\bar{S} \hat{v}(k-1) - \bar{v}(k)}{\bar{S} \omega(k-1)} \right)), & k \notin H_q \\ \bar{S} \hat{v}(k-1), & k \in H_q \end{cases} \quad (14)$$

in which $Q_v(\cdot)$ is the vector form of (4), $\omega(k) \in \mathbb{R}^{n_v}$ is a scaling vector for quantizing $\bar{v}(k)$, “ \circ ” is the element-wise multiplication and “ \oslash ” is the element-wise division. The computation of $\omega(k)$ in (14) is given as follows:

$$\begin{cases} \omega(k) = \begin{cases} \tilde{S}H\omega(k-1), & k \notin H_q \\ \tilde{S}\omega(k-1), & k \in H_q \end{cases} \\ H = \text{diag}(2^{-R_1}I_1, 2^{-R_2}I_2, \dots, 2^{-R_p}I_p) \in \mathbb{R}^{n_v \times n_v} \end{cases} \quad (15)$$

where the block diagonal matrix $\tilde{S} = \text{diag}(\tilde{S}_1, \dots, \tilde{S}_p) \in \mathbb{R}^{n_v \times n_v}$. If r corresponds to a real eigenvalue $\lambda_r \in \mathbb{R}$, then $\tilde{S}_r = \bar{S}_r$ in (7). Otherwise, \tilde{S}_r takes

$$\tilde{S}_r = \begin{bmatrix} \zeta_r I_2 & O \\ & \zeta_r I_2 & O \\ & & \ddots \\ & & & \zeta_r I_2 \end{bmatrix} \in \mathbb{R}^{2n_r \times 2n_r}, O = \begin{bmatrix} 1 & 1 \\ 1 & 1 \end{bmatrix}. \quad (16)$$

Similar to [8], the parameter R_r ($r = 1, \dots, p$) in H is the number of bits for the quantization process corresponding to \bar{S}_r . If R_r is determined, then \mathcal{R}_l in (4) is determined as well. At last, we assume that the initial conditions in the encoding and decoding systems are identical and satisfy

$$\hat{v}_l(0) = 0, \omega_l(0) > |\bar{v}_l(0)|, l = 1, 2, \dots, v \quad (17)$$

where $\hat{v}_l(k) \in \mathbb{R}$ and $\omega_l(k) \in \mathbb{R}$ denote the l -th element in vectors $\hat{v}(k) = [\hat{v}_1(k) \dots \hat{v}_v(k)]^T$ and $\omega(k) = [\omega_1(k) \dots \omega_v(k)]^T$, respectively.

4 Stability analysis

Define vectors $\bar{z}(k) := [\bar{z}_1^T(k) \dots \bar{z}_N^T(k)]^T$, $\hat{z}(k) := [\hat{z}_1^T(k) \dots \hat{z}_N^T(k)]^T$ and $\delta(k) := \bar{z}(k) - \mathbf{1}_N \otimes \bar{v}(k)$. Define errors $e_z(k) := \bar{z}(k) - \hat{z}(k)$ (of estimating $\bar{z}(k)$) and $e_v(k) := \hat{v}(k) - \bar{v}(k)$ (of estimating $\bar{v}(k)$). Define matrices $G := \bar{S}_N - (\mathcal{L}_G + \mathcal{D}) \otimes \bar{K}$, $\bar{S}_N := I_N \otimes \bar{S}$, $W := \mathcal{D} \otimes \bar{K}$, $P := (\mathcal{L}_G + \mathcal{D}) \otimes \bar{K}$ and $Z := \bar{S}_N + (\mathcal{L}_G + \mathcal{D}) \otimes \bar{K}$. We define $\alpha(k) := \delta(k)/\theta_k$, $\xi_z(k) := e_z(k)/\theta_k$ and $\xi_v(k) := e_v(k)/\theta_k$. Accordingly, we obtain the dynamics of $\alpha(k)$ and $\xi_z(k)$ in four cases as follows. The dynamics of $\xi_v(k)$ will be analyzed later.

Case I: $k+1 \notin H_q$ and $k \notin H_q$

$$\alpha(k+1) = \frac{G}{\gamma_1} \alpha(k) + \frac{P}{\gamma_1} \xi_z(k) - \frac{W}{\gamma_1} (\mathbf{1}_N \otimes \xi_v(k)) \quad (18a)$$

$$\begin{aligned} \xi_z(k+1) &= \frac{Z}{\gamma_1} \xi_z(k) - \frac{P}{\gamma_1} \alpha(k) - \frac{W}{\gamma_1} (\mathbf{1}_N \otimes \xi_v(k)) \\ &\quad - \frac{1}{\gamma_1} Q (Z \xi_z(k) - P \alpha(k) - W (\mathbf{1}_N \otimes \xi_v(k))) \end{aligned} \quad (18b)$$

Case II: $k+1 \notin H_q$ and $k \in H_q$

$$\alpha(k+1) = \frac{\bar{S}_N}{\gamma_1} \alpha(k) \quad (19a)$$

$$\xi_z(k+1) = \frac{\bar{S}_N}{\gamma_1} \xi_z(k) - \frac{1}{\gamma_1} Q (\bar{S}_N \xi_z(k)) \quad (19b)$$

Case III: $k+1 \in H_q$ and $k \notin H_q$

$$\alpha(k+1) = \frac{G}{\gamma_2} \alpha(k) + \frac{P}{\gamma_2} \xi_z(k) - \frac{W}{\gamma_2} (\mathbf{1}_N \otimes \xi_v(k)) \quad (20a)$$

$$\xi_z(k+1) = \frac{Z}{\gamma_2} \xi_z(k) - \frac{P}{\gamma_2} \alpha(k) - \frac{W}{\gamma_2} (\mathbf{1}_N \otimes \xi_v(k)) \quad (20b)$$

Case IV: $k+1 \in H_q$ and $k \in H_q$

$$\alpha(k+1) = \frac{\bar{S}_N}{\gamma_2} \alpha(k) \quad (21a)$$

$$\xi_z(k+1) = \frac{\bar{S}_N}{\gamma_2} \xi_z(k). \quad (21b)$$

The next proposition specifies the ranges of γ_1 , γ_2 and the value of $(2R_f + 1)\sigma$ preventing the saturation of (3). Its proof with C_1 and C_2 is provided in the Appendix.

Proposition 1 Suppose there exists a $E_v \in \mathbb{R}_{>0}$ such that $\|\xi_v(k)\|_\infty \leq E_v$. Choose the zooming-in factor by $\rho(G) < \gamma_1 < 1$, the zooming-out factor by $\gamma_2 > \rho(S)$ and $\theta_0 \geq C_{x_0} \gamma_1 / \sigma$. Under DoS attacks in Assumptions 1 and 2, the quantizer (3) is free of saturation if

$$\begin{aligned} &(2R_f + 1)\sigma \\ &\geq C_2 \|\bar{S}_N\| \left(\|Z\| \sqrt{Nv} \frac{\sigma}{\gamma_1} + \|P\| C_1 + \|W\| \sqrt{Nv} E_v \right). \quad \blacksquare \end{aligned}$$

Remark 2 Lemma 1 is necessary to obtain “tight” γ_1 and γ_2 . Otherwise, the matrices on the diagonals of \bar{S}_N and \bar{G} (in (29)) shall be S and $S - \bar{\lambda}_i \bar{K}$, respectively, which are not necessarily upper-triangular. Then, the stabilization of the switched system regulated by \bar{S}_N and \bar{G} can be subject to dwell time constraints. Consequently, γ_1 and γ_2 can be much more conservative in order to compensate the state “jumps” of the switched system as in [27]. Alternatively, if one seeks to obtain a less conservative zooming-out parameter, DoS frequency (regulating the switching frequency) should be upper bounded in order to ensure that the quantizer is not saturated and consensus is achieved [28]. \blacksquare

In Proposition 1, by properly selecting γ_1 and γ_2 , we have provided the value of $(2R_f + 1)\sigma$ for the unsaturation of quantizer (3), by supposing $\xi_v(k)$ upper bounded. In the following proposition, we provide the conditions to ensure an upper bounded $\xi_v(k)$, namely a finite E_v .

Proposition 2 Supposing that γ_2 is selected as in Proposition 1, we have the following results:

- The quantizer for the leader’s state in (4) is free of overflow for all k .
- If γ_1 satisfying Proposition 1 is given, then R_r needs to satisfy $2^{R_r} > \zeta_r / \gamma_1$ so that E_v is finite.
- If $R_r > \log_2 \zeta_r$ is pre-given, then E_v is finite if γ_1 satisfies $\max\{\rho(\bar{G}), \zeta_r / 2^{R_r}\} < \gamma_1 < 1$ with \bar{G} in (29).

Proof. Let $e_{vl}(k)$ denote the l -th element of vector $e_v(k)$. To prove a), we will show $|e_{vl}(k)| \leq \omega_l(k)$, which implies quantizer unsaturation in view of (4). If $k = 1 \notin H_q$, then by (14) one has

$$e_v(1) = \bar{S} \left(e_v(0) - \omega(0) \circ Q_v \left(\frac{e_v(0)}{\omega(0)} \right) \right). \quad (22)$$

Note that $|e_{vl}(0)| \leq \omega_l(0)$ implied by (17). Then according to (5), element-wise inequality of (22) yields

$$|e_{vl}(1)| \leq |\tilde{S}_l| H \omega(0) \leq \tilde{S}_l H \omega(0) = \omega_l(1) \quad (23)$$

in which $|\tilde{S}_l|$ is the l -th row of $|\tilde{S}|$, and \tilde{S}_l is the l -th row of \tilde{S} . Here, $|\tilde{S}|$ is a matrix in which the elements are the absolute values of the corresponding elements in \tilde{S} . If $k = 1 \in H_q$, we have $e_v(1) = \tilde{S}e_v(0)$ by (14). Following a similar element-wise analysis as in (23), one has

$$|e_{vl}(1)| \leq |\tilde{S}_l| [|e_{v1}(0)| \cdots |e_{vv}(0)|]^T \leq \tilde{S}_l \omega(0) = \omega_l(1). \quad (24)$$

By the above analysis, we have shown that if overflow does not occur at $k = 0$, then no matter $k = 1$ is corrupted by DoS or not, overflow cannot occur. By induction, one can confirm that overflow does not occur for all k .

To prove b) and c), we first analyze the dynamics of

$$\xi_{vl}(k) = \frac{e_{vl}(k) \omega_l(k)}{\omega_l(k) \theta(k)} \quad (25)$$

where $\xi_{vl}(k)$ is the l -th element in $\xi_v(k)$. We have shown that $|e_{vl}(k)|/\omega_l(k) \leq 1$ in a). In order to ensure $\xi_{vl}(k)$ is bounded, one needs to ensure that $w_l(k)/\theta(k)$ is upper bounded, namely bounded $w(k)/\theta(k)$ in vector form. Let $\bar{\omega}(k) := \omega(k)/\theta_k$. In the absence of DoS, by (13) and (15), one has

$$\bar{\omega}(k+1) = \frac{\tilde{S}H}{\gamma_1} \bar{\omega}(k). \quad (26)$$

It is clear that if b) or c) holds, then $\rho(\tilde{S}H/\gamma_1) < 1$. In the presence of DoS, we have

$$\bar{\omega}(k+1) = \frac{\tilde{S}}{\gamma_2} \bar{\omega}(k) \quad (27)$$

where $\rho(\tilde{S}/\gamma_2) < 1$ since $\gamma_2 > \rho(\tilde{S}) = \rho(\tilde{S})$ in Proposition 1. Because $\tilde{S}H$ and \tilde{S} are upper-triangular matrices, by the stabilization of switched systems, one can confirm that $\bar{\omega}(k)$ is bounded, and hence there exists a positive and finite E_v such that $\|\xi_v(k)\|_\infty \leq E_v$ in view of (25). ■

Remark 3 Proposition 2 shows that due to the design of $\omega(k)$ and \tilde{S} therein, the quantizer (4) is free of overflow for any R_r . However, an inappropriate R_r can induce saturation problems to the quantizer (3). For instance, arbitrarily approaching the minimum data rate for R_r is not enough. Even if some followers can estimate $\bar{v}(k)$ under the minimum R_r and quantizer (4) is not saturated, the quantizer (3) may have overflow problem. Specifically, suppose that R_r is sufficiently close to the minimum data rate $\log_2 \zeta_r$. Under such a R_r , the quantization error of leader's state e_v converges to zero in the absence of DoS attacks. However, such a R_r does not necessarily satisfy $R_r > \log_2(\zeta_r/\gamma_1)$ in Proposition 2 b). The violation of Proposition 2 b) can make the dynamics of (26) unstable and consequently E_v infinitely large. By Proposition 2, if E_v is unbounded, any finite-range quantizer (3) for followers' state has the overflow problem. To solve the problem, there are two options. The first option is selecting a larger R_r , i.e., satisfying b) in Proposition 2 for a given γ_1 . As a second option, if one would like to get close to the minimum R_r [33], then a γ_1 sufficiently close to 1 is needed as indicated in c). As will

be shown in Theorem 1, when R_r approaches the minimum data rate, one gets a poor resilience.

We emphasize that if one adopts an identical quantization mechanism for the leader's and followers' state as in [27] (as in (3), (12) and (13)), it is difficult to make R_r tight, and the gap between R_r and the minimum data rate is invisible. If one adopts an identical quantization mechanism for the leader's and followers' state as in (4), (14), (15), then designing the scaling parameter to ensure the followers' state satisfying $|e_l/\omega_l|$ in (5) is one of the major challenges, which will be left for future research. ■

As a special case, if the dimension of the \tilde{S}_r corresponding to the spectral radius is 1, the result in Proposition 2 b) can be relaxed to $2^{R_r} \geq \zeta_r/\gamma_1$. Note that if the dimension of the \tilde{S}_r corresponding to the spectral radius is larger than 1, such a relaxation can make (26) unstable. Similarly, if the dimension of the \tilde{S}_r corresponding to the spectral radius is 1, one can let $\gamma_2 = \rho(\tilde{S})$.

Note that Proposition 2 cannot imply tracking control under DoS. The following main result characterizes the system's resilience of tracking control under DoS attacks.

Theorem 1 Suppose that γ_1 and R_r satisfy b) or c) in Proposition 2, and γ_2 satisfies Proposition 1. Then, one can achieve the tracking control if DoS attacks satisfy

$$\begin{aligned} \frac{1}{T} + \frac{\Delta}{\tau_D} &< 1 - \frac{\log_2 \gamma_2}{\log_2 \gamma_2 - \log_2 \gamma_1} \\ &< 1 - \frac{\log_2 \gamma_2}{\log_2 \gamma_2 - \log_2 \frac{\zeta_r}{2^{R_r}}}. \end{aligned} \quad (28)$$

Proof. For achieving tracking control, it is necessary that $\delta(k) \rightarrow 0$ as $k \rightarrow \infty$. This can be obtained by $\theta_k \rightarrow 0$ in view of $\delta(k) = \theta_k \alpha(k)$, in which one can confirm that $\|\alpha(k)\|$ is upper bounded by following a similar analysis in the proof of Proposition 1. If DoS attacks satisfy the first inequality in (28), then one has $\theta_k \rightarrow 0$ [27]. By Proposition 2, one can infer that (R_r, γ_1) satisfies $\gamma_1 > \zeta_r/2^{R_r}$. Thus, one can obtain the second inequality in (28).

Now we show $y(k) \rightarrow v(k)$. Let $A := \text{diag}(A_1, \dots, A_N)$, and B, K, F and V take the similar form being block diagonal matrices. Let $E(k) := I_N \otimes E(k)$ and $T := I_N \otimes T$. Then, in view of Assumption 3 and $p(k) := x(k) - Fv(k)$, one has $p(k+1) = (A + BK)p(k) + B(KF - V)(\mathbf{1}_N \otimes v(k) - z(k)) = (A + BK)p(k) + B(KF - U)T^{-1}E^{-1}(k)(\mathbf{1}_N \otimes \bar{v}(k) - \bar{z}(k))$, in which we have shown that $\bar{z}(k) - \mathbf{1}_N \otimes \bar{v}(k) = \delta(k) \rightarrow 0$. Since $\rho(A + BK) < 1$ and $\|T^{-1}E^{-1}(k)\|$ bounded, one can verify that $p(k) \rightarrow 0$ as $k \rightarrow \infty$, and hence $Cp(k) = Cx(k) - CFv(k) = y(k) - v(k) \rightarrow 0$. ■

Remark 4 a) By (28), it is clear that the resilience depends on the leader-follower communication and inter-follower communication. Small γ_1 and γ_2 , and a large R_r can improve the system's resilience against DoS. Without affecting the main idea of the paper, we let γ_2 infinitely approach $\rho(S)$. This is a significant improvement compared with [27, 28].

b) If one selects a sufficiently large R_r for leader-follower quantized communication, e.g., $\zeta_r/2^{R_r} < \rho(G) < \gamma_1$, then

the quantized communication among the followers is the bottleneck of resilience. In other words, large γ_1 and γ_2 lead to poor resilience no matter how large is R_r . Mathematically, this can be confirmed by (28). We provide an intuitive explanation. Suppose that one chooses a R_r large enough such that the second inequity in (28) is infinitely close to 1. This implies that leader's state has almost no quantization effects, and the leader's direct neighbors can obtain the leader's state by only one successful transmission. Subsequently, communication between the leader and its direct followers is not necessary since the followers can perfectly estimate $v(k)$ locally. The rest to be done is that the followers who have $v(k)$ should "deliver" $v(k)$ to the other followers via the follower-follower communication. Then, it is intuitive to see that, now the ability of cooperative control among followers under DoS becomes the bottleneck, i.e., γ_1 and γ_2 .

c) The quantized communication between the leader and followers is the "ceiling" of resilience if one selects a small R_r , e.g., $\zeta_r/2^{R_r}$ is close to 1. In this case, tuning the followers' parameters cannot help much because γ_1 is lower bounded by $\zeta_r/2^{R_r}$ for preventing quantizer overflow in view of c) in Proposition 2. In order to prevent further resilience degradation induced by the quantized communication among followers (the first inequality in (28)), one needs to make $\gamma_1 \rightarrow \zeta_r/2^{R_r}$ from the right. Then, one can verify that the right hand-side of the first inequality in (28) approaches that of the second inequality (the "ceiling"). One can still try to improve $\gamma_1 < \zeta_r/2^{R_r}$ such that the first inequality goes beyond the "ceiling" determined by R_r . However, this can cause quantizer overflow problem to (3) due to unbounded E_v (see the bottom plot in Fig. 3), which violates the first control objective.

d) Following a)-c), if one has selected a γ_2 close to $\rho(S)$, a small γ_1 close to $\rho(G)$ and a $R_r > \log_2 \zeta_r/\gamma_1$, then there is not much room for improving the resilience by quantized controller design. This is because S (determining γ_2) can depend on the inherent properties of the leader, and G (determining γ_1) depends on S and communication topology. They together determine the bottleneck. One can attempt to find a \bar{K} minimizing $\rho(G)$, but this is out of the scope of our paper. ■

By the proof of Theorem 1, the dynamics of $p(k)$ determines the convergence rate of $y(k) - v(k)$. It is straightforward that $\|\bar{z}(k) - \mathbf{1}_N \otimes \bar{v}(k)\| = \|\delta(k)\| = \|\theta_k \alpha(k)\| \leq \theta_k C$ influences the convergence speed, where $C > 0$ denotes an upper bound of $\|\alpha(k)\|$. Now, one can see that the convergence speed mainly depends on θ_k . In view of (13), a small γ_1 satisfying $\max\{\rho(\bar{S} - \tilde{\lambda}_i \bar{K})\}_{i \in \mathcal{N}} < \gamma_1 < 1$ and a small $\gamma_2 > \rho(S)$, and less times of $k \in H_q$ can lead to a "fast" convergence of θ_k , which essentially depends on the dynamics of \bar{S} , the eigenvalues of $\mathcal{L} + \mathcal{D}$ and the number of packet losses induced by DoS attacks. Fast converge rate also requires more data rate. This can be confirmed by Proposition 1 and Proposition 2 b). Otherwise, quantizer overflow can occur. To maximize the convergence speed, in general, one should improve the communication topology, select a \bar{K}

minimizing $\max\{\rho(\bar{S} - \tilde{\lambda}_i \bar{K})\}_{i \in \mathcal{N}}$, a γ_1 sufficiently close to $\max\{\rho(\bar{S} - \tilde{\lambda}_i \bar{K})\}_{i \in \mathcal{N}}$, and a large R_r satisfying Proposition 2.

One can almost recover the number of quantization levels for homogeneous multi-agent systems by making the heterogeneous quantization mechanisms in this paper homogeneous by letting $E_v = \sigma/\gamma_1$. By "almost", we mean that the values can be different due to parameter selections and dwell time constraints in [27]. Meanwhile, the inequalities in (28) characterizing the resilience recover to that in [27].

If the communication network is free of DoS attacks but subject to quantization, the zooming-out process is not needed and the problem recovers to the classic quantized leader-follower consensus. Note that if one applies heterogeneous quantization mechanisms as proposed in this paper, one still needs b) or c) in Proposition 2 to hold. Otherwise, follower's quantizer can have overflow problem. Our result can also recover to that of quantization-free network under DoS attacks, namely choosing $\gamma_1 = \max\{\rho(\bar{S} - \tilde{\lambda}_i \bar{K})\}_{i \in \mathcal{N}}$ and $\gamma_2 = \rho(S)$. However, such γ_1 and γ_2 can lead to infinite quantization levels due to infinite $\alpha(k)$ and E_v caused by $\rho(\bar{S}_N/\gamma_2) = \rho(G/\gamma_1) = 1$ (see the Appendix and (27), respectively). This is consistent with quantized consensus for homogeneous multi-agent systems under DoS attacks.

5 Simulation

In this section, we present two examples. Example 1 is mainly for the verification of the ceiling and bottleneck effects, and Example 2 is the application of our control scheme to the tracking control of mobile robots.

Example 1: We consider a multi-agent system with one leader and four followers. The dynamics of the leader and followers is regulated by $S = [1.1052 \ 0.1105; 0 \ 1.1052]$, and $A_i = [0 \ 1; 0 \ 0]$, $B_i = [1.1052 \ -0.8895; 0 \ 1.1052]$ and $C_i = [1 \ 0.5; 0 \ 1]$, respectively. The interaction between the leader and followers is represented by $\mathcal{D} = \text{diag}(1, 0, 1, 0)$. The Laplacian matrix of the graph for inter-followers' communication follows that in [28]. The feedback gain in (9) is selected as $\bar{K}_i = -0.1I_2$ and the design parameter in (11) is selected as $K = 0.4683I_2$. The transmission interval between k and $k + 1$ is $\Delta = 0.1s$.

One can obtain $\rho(G) = 0.9161$ and $\rho(S) = 1.1052$. Then we select $\gamma_1 = 0.92$ and $\gamma_2 = 1.10521$ following Proposition 1. We select $R_1 = 1$ according to Proposition 2. By Proposition 1, we obtain $(2R_f + 1)\sigma > 7.3638 \cdot 10^{14}$, which can be encoded by 50 bits. The theoretical sufficient bound of DoS attacks computed by Theorem 1 is 0.4546. We consider a sustained DoS attack with variable period and duty cycle, generated randomly. Over a simulation horizon of 20s, the DoS signal yields $|\Xi(0, 20)| = 5.7s$ and $n(0, 20) = 42$. This corresponds to values (averaged over 20s) of $\tau_D \approx 0.4762$ and $1/T \approx 0.2850$, and hence $\Delta/\tau_D \approx 0.15$ and $\Delta/\tau_D + 1/T \approx 0.495$. Since our result regarding tolerable DoS attacks is a sufficient condition, one can see from the first plot in Figure 2 that the tracking control is achieved. We mention that the variables to be quantized in $Q(\cdot)$ in the simulation are between -7.65 and 9.2 (5 bits per state),

which is much smaller than the theoretical result, i.e., $9.2 \ll 7.3638 \cdot 10^{14}$. The theoretical result is conservative since we have selected γ_1 and γ_2 very close to their lower bounds and this can lead to large C_1 , C_2 and E_v .

Now we show the bottleneck effect. We select $\gamma_1 = 0.97$ and let γ_2 be the same. According to Proposition 2 b), one sees that $R_1 = 1$ still satisfies the inequalities. However, for the same DoS pattern studied above, one can see from the second plot in Figure 2 that the tracking error diverges. Note that the value of R_1 does not change and hence the ‘‘ceiling’’ does not change (the second inequality in (28)). However, the first inequality in (28) becomes smaller under a smaller γ_1 , which is actually the bottleneck of resilience causing state divergence. In this example, one still needs 50 bits for encoding a state because one selects a tight γ_2 for the pair $(\rho(S)/\gamma_2, \rho(G)/\gamma_1)$, and $\rho(S)/\gamma_2$ determines the lower rate for iteration during the computation of C_1 , C_2 and E_v . In the simulation, we actually have $-8 \leq \|Q(\cdot)\|_\infty \leq 8$ (5 bits per state), though the tracking control fails due to the bottleneck effect.

In the following, we show the ceiling effect caused by R_1 . In the simulation example above, we have shown that $R_1 = 1$ is already sufficiently large, i.e., $\zeta_1/2^{R_1} < \rho(G)$. Thus, we verify the ceiling effect by an academic value $R_1 = 0.2$. According to Proposition 2 c), one can choose $\gamma_1 = 0.97$. Similarly, we let $\gamma_2 = 1.10521$. Under this setting, we can see from the first plot of Figure 3 that tracking is achieved. Note that both R_1 and γ_1 now are smaller than the values in the previous examples, and hence the sufficient bound of tolerable DoS attacks is smaller. To recover the resilience to that in previous examples, we enlarge γ_1 for mitigating the bottleneck, i.e., $\gamma_1 = 0.93$ and $R_1 = 0.2$. However, as we presented in Proposition 2 and (28), only improving the bottleneck (beyond the ‘‘ceiling’’) can cause overflow problems of follower’s quantizers. This is shown in the second plot in Figure 3, which implies that the variables to be quantized by $Q(\cdot)$ diverge. This implies that when R_1 is fixed and small, R_1 will determine the upper bound of resilience. One cannot further improve the resilience by violating the ceiling effect. Otherwise, the quantizer (3) will have saturation problems.

Example 2: In this example, we apply our control scheme to the tracking control of mobile robots under quantization and DoS attacks. The dynamics of four follower mobile robots is taken from [37] as $\dot{x}_{i1}(t) = x_{i2}(t)$, $\dot{x}_{i2}(t) = -c_i x_{i2}(t) + u_i(t)$, in which $x_{i1}(t)$ and $x_{i2}(t)$ denote the position and velocity, respectively, with $i = 1, 2, 3, 4$, and $c_i = 0.2$ is the friction parameter. The virtual leader is an autonomous system with dynamics $\dot{v}(t) = [0 \ 1; 0 \ 0]v(t)$ and the elements in $v(t) = [v_1(t) \ v_2(t)]^T$ denote the position and velocity. Let $y_i(t) = [x_{i1}(t) \ x_{i2}(t)]^T$ for $i = 1, 2, 3, 4$. It is simple to obtain the system matrices for sampled-data dynamics with sampling interval $\Delta = 0.1s$: $A_i = [1.0000 \ 0.0990; 0 \ 0.9802]$, $B_i = [0.004967; 0.09901]$ for followers $i = 1, 2, 3, 4$ and $S = [1 \ 0.1; 0 \ 1]$ for the leader. The communication topology is illustrated in the top picture in Figure 4. We select $K_i = [-77.2624 \ -13.5990]$ and $\bar{K} = 0.42I_2$. One can verify that $\rho(G) = 0.9493$ and

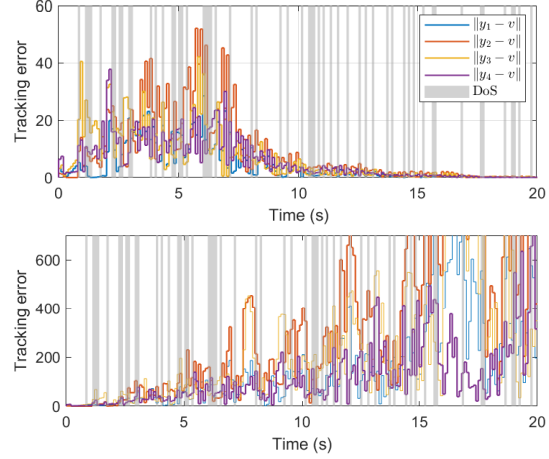


Fig. 2. Top: Time response of tracking errors ($\gamma_1 = 0.92$); Bottom: Time response of tracking errors ($\gamma_1 = 0.97$) and the legend follows that in the top plot.

$\rho(S) = 1$. Then we select $\gamma_1 = 0.95$, $\gamma_2 = 1.01$ and $R_1 = 1$ by Proposition 1. By Theorem 1, if $1/T + \Delta/\tau_D < 0.8375$, tracking control can be achieved. Similarly to Example 1, DoS attacks are generated randomly with $|\Xi(0.50)| = 29.6s$ and $n(0, 50) = 122$ as shown in the middle picture in Figure 4, which yield $1/T + \Delta/\tau_D \approx 0.836$. It satisfies the bound of tolerable DoS attacks, i.e., $0.836 < 0.8375$. The time response of tracking errors are provided in the middle picture of Figure 4, which presents the success of tracking control under DoS by $\|y_i - v\| \rightarrow 0$.

We compare the performance of tracking control in the presence and absence of quantization. To make the comparison clear, DoS attacks are not considered. Moreover, we assume that the virtual leader increases its speed by 1m/s at 25s and the followers should track the new speed as well as the position. As shown in the last plot in Figure 4, the tracking errors converge to 0 in $[0, 25]s$ and $(20, 50]s$ with and without quantization. In particular, by the simulation curves in $(25, 50]s$, the convergence speed under quantization is close to the one without quantization. To further improve their convergence speeds, one needs to improve the communication topology, e.g., by unitizing the one in Example 1 and obtaining $\rho_{\text{new}}(G) = 0.8304$. By the new $\rho_{\text{new}}(G)$, it is straightforward that the convergence speed without quantization is faster and the one under quantization is also faster since one can select a smaller γ_1 .

6 Conclusions and future research

This paper studied tracking control of heterogeneous multi-agent systems under DoS attacks and state quantization. We have designed heterogeneous quantization mechanisms for the leader’s and followers’ state. With the dynamical quantized controllers with zooming-in and out capabilities, and proper data rate, we have shown that the quantizers are free of saturation under DoS attacks. Our results revealed the bottleneck effect of resilience: if one selects a ‘‘large’’ data rate for leader-follower quantized communication, further enlarging it cannot improve the resilience. Then, the inter-follower quantized communication determines the re-

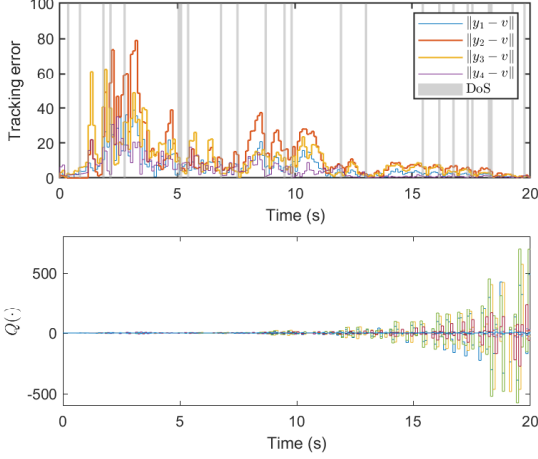


Fig. 3. Top: Time response of tracking errors; Bottom: The output of $Q(\cdot)$.

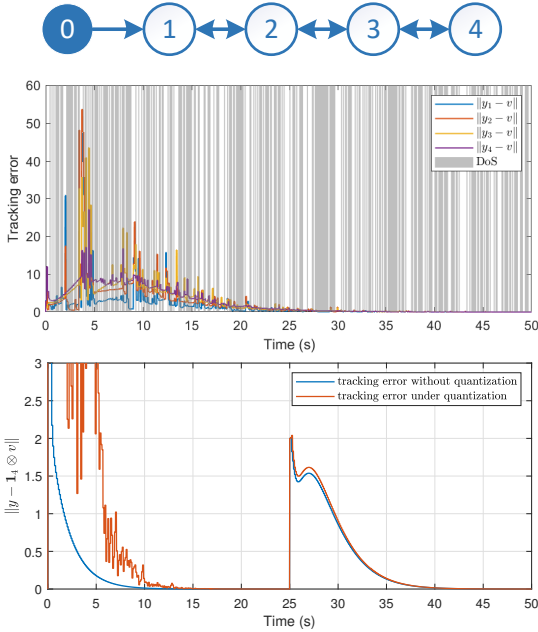


Fig. 4. Top: Communication topology with agent 0 being the leader and agents 1-4 being the followers; Middle: Time response of tracking errors under DoS; Bottom: Time response of tracking errors without and under quantization with $y := [y_1^T \ y_2^T \ y_3^T \ y_4^T]^T$.

silence. We also presented the ceiling effect of resilience: by tuning the quantized controllers of followers, one can at most improve the resilience to the level determined by the data rate of leader-follower quantized communication. Otherwise, overflow of followers' state quantizer can occur.

For the directions of future research, it is interesting to consider the presence of noise. Then the dynamics of the tracking error is expected to be practically stable [32]. One can also design distributed scaling parameters such that each follower agent can have individual zooming-in and out factors. Moreover, it is useful to design controllers that can tolerate communication delays [38], uncertainties [39] and accelerate consensus speed [40].

Appendix–Proof of Proposition 1

By Cases I–IV in Section 4, the evolution of α along with the sequence of successful steps $\{s_r\} \subseteq \{k\}$ follows: $\alpha(s_r) = (\frac{\bar{S}_N}{\gamma_2})^{m_{r-1}} \frac{\bar{G}}{\gamma_1} \alpha(s_{r-1}) + (\frac{\bar{S}_N}{\gamma_2})^{m_{r-1}} (\frac{P}{\gamma_1} \xi_z(s_{r-1}) - \frac{W}{\gamma_1} (\mathbf{1}_N \otimes \xi_v(s_{r-1})))$, where $m_{r-1} \geq 0$ denote the number of unsuccessful transmission between s_{r-1} and s_r . There exists a unitary matrix U such that $U^T(\mathcal{L}_G + \mathcal{D})U$ is an upper-triangular matrix whose diagonals are $\tilde{\lambda}_i$. Then it is simple to obtain that

$$\bar{G} := (U \otimes I_v)^T G (U \otimes I_v) = \begin{bmatrix} \bar{S} - \tilde{\lambda}_1 \bar{K} & * & * \\ & \ddots & * \\ & & \bar{S} - \tilde{\lambda}_N \bar{K} \end{bmatrix}. \quad (29)$$

Recall that \bar{S} is an upper-triangular matrix, then we assume that there exists an upper-triangular \bar{K} such that $\bar{S} - \tilde{\lambda}_i \bar{K}$ is Schur stable for $i = 1, \dots, N$.

Define vectors $\bar{\alpha}(k) := (U \otimes I_v)^T \alpha(k)$, $\bar{\xi}_z(k) := (U \otimes I_v)^T \frac{P}{\gamma_1} \xi_z(k)$ and $\bar{\xi}_v(k) := (U \otimes I_v)^T \frac{W}{\gamma_1} (\mathbf{1}_N \otimes \xi_v(k))$. Then, one has $\bar{\alpha}(s_r) = (\frac{\bar{S}_N}{\gamma_2})^{m_{r-1}} \frac{\bar{G}}{\gamma_1} \bar{\alpha}(s_{r-1}) + (\frac{\bar{S}_N}{\gamma_2})^{m_{r-1}} (\bar{\xi}_z(s_{r-1}) - \bar{\xi}_v(s_{r-1}))$, which is obtained by the fact that $(U \otimes I_v)^T$ and $\bar{S}_N^{m_{r-1}}$ are commuting matrices. Let s_{-1} denote the step $k = 0$. Then we have $\|\alpha(s_{-1})\| = \|\bar{\alpha}(0)\| \leq 2\sqrt{N}n_v \frac{C_{x0}}{\theta_0}$, $\|\bar{\xi}_z(s_r)\| \leq \|P\| \sqrt{N}n_v \frac{\sigma}{\gamma_1}$ and $\|\bar{\xi}_v(s_r)\| \leq \|W\| \sqrt{N}n_v \frac{E_v}{\gamma_1}$, and $\rho(\bar{G}/\gamma_1) < 1$ and $\rho(\bar{S}_N/\gamma_2) < 1$ by the selections of γ_1 and γ_2 . By the stabilization of switched systems, there exists a positive real C_1 such that $\|\bar{\alpha}(s_r)\| \leq C_1$. In particular, \bar{S}_N and \bar{G} are upper-triangular, which implies there are no dwell-time constraints.

To analyze the overflow problem, i.e., the lower bound of $(2R_f + 1)\sigma$, one needs to investigate $\|\frac{\bar{z}(k) - \bar{S}_N \bar{z}(k-1)}{\theta_{k-1}}\|_\infty$ by (12). At $s_r + 1$, one has $\|(\bar{z}(s_r + 1) - \bar{S}_N \bar{z}(s_r))/\theta_{s_r}\|_\infty = \|Z \xi_z(s_r) - P \alpha(s_r) - W (\mathbf{1}_N \otimes \xi_v(s_r))\|_\infty \leq \|Z \xi_z(s_r) - P \alpha(s_r) - W (\mathbf{1}_N \otimes \xi_v(s_r))\| \leq (2R_f + 1)\sigma$ which implies unsaturation of follows' quantizer $q_{R_f}(\cdot)$. For the step of $s_r + 2$, if $s_r + 1$ is a successful transmission step, one can follow the similar analysis presented in the step of $s_r + 1$ and shows quantizer unsaturation. If $s_r + 1$ is not a successful transmission step, then one has $\|\frac{\bar{z}(s_r+2) - \bar{S}_N \bar{z}(s_r+1)}{\theta_{s_r+1}}\|_\infty = \|\bar{S}_N \xi_z(s_r + 1)\|_\infty \leq (2R_f + 1)\sigma$, in which we have used $\|\xi_z(s_r + 1)\|_\infty \leq \|Z \xi_z(s_r) - P \alpha(s_r) - W (\mathbf{1}_N \otimes \xi_v(s_r))\|_\infty$. By induction, if the transmissions at $s_r + m - 1$ are all failed, then for $s_r + m$ ($m \geq 2$), one has $\|\frac{\bar{z}(s_r+m) - \bar{S}_N \bar{z}(s_r+m-1)}{\theta_{s_r+m-1}}\|_\infty = \|\bar{S}_N \xi_z(s_r + m - 1)\|_\infty = \|\bar{S}_N \left(\frac{\bar{S}_N}{\gamma_2}\right)^{m-2} \xi_z(s_r + 1)\|_\infty \leq (2R_f + 1)\sigma$, in which $\rho(\bar{S}_N/\gamma_2) < 1$ such that $\|(\bar{S}_N/\gamma_2)^k\| \leq C_2 \in \mathbb{R}_{>0}$. By the above analysis, one can see that the quantizer $q_{R_f}(\cdot)$ does not saturate at s_r , $s_r + 1$ and $s_r + m$ ($m \geq 2$), which implies quantizer unsaturation at all k . ■

References

- [1] F. Bullo. *Lectures on Network Systems*. Kindle Direct Publishing, 2019.
- [2] A. Cardenas, S. Amin, B. Sinopoli, A. Giani, A. Perrig, and S. S. Sastry. Challenges for securing cyber physical systems. In *Workshop on future directions in cyber-physical systems security*, volume 5, 2009.
- [3] K. You and L. Xie. Minimum data rate for mean square stabilization of discrete lti systems over lossy channels. *IEEE Transactions on Automatic Control*, 55(10):2373–2378, 2010.
- [4] C. De Persis and P. Tesi. Input-to-state stabilizing control under Denial-of-Service. *IEEE Transactions on Automatic Control*, 60(11):2930–2944, 2015.
- [5] A. Lu and G. Yang. Input-to-state stabilizing control for cyber-physical systems with multiple transmission channels under Denial of Service. *IEEE Transactions on Automatic Control*, 63(6):1813–1820, 2017.
- [6] T. Pierron, T. Árauz, J. M. Maestre, A. Cetinkaya, and C. S. Maniu. Tree-based model predictive control for jamming attacks. In *European Control Conference*, pages 948–953, 2020.
- [7] S. Amin, A. Cardenas, and S. S. Sastry. Safe and secure networked control systems under Denial-of-Service attacks. *Hybrid Systems: Computation and Control*, pages 31–45, 2009.
- [8] S. Feng, A. Cetinkaya, H. Ishii, P. Tesi, and C. De Persis. Networked control under DoS attacks: Tradeoffs between resilience and data rate. *IEEE Transactions on Automatic Control*, 66(1):460–467, 2021.
- [9] A. Cetinkaya, H. Ishii, and T. Hayakawa. Analysis of stochastic switched systems with application to networked control under jamming attacks. *IEEE Transactions on Automatic Control*, 64(5):2013–2028, 2019.
- [10] C. Bhowmick and S. Jagannathan. Availability-resilient control of uncertain linear stochastic networked control systems. In *American Control Conference*, pages 4016–4021, 2020.
- [11] K. Ding, X. Ren, D. Quevedo, S. Dey, and L. Shi. DoS attacks on remote state estimation with asymmetric information. *IEEE Transactions on Control of Network Systems*, 6(2):653–666, 2018.
- [12] H. S. Foroush and S. Martínez. On triggering control of single-input linear systems under pulse-width modulated DoS jamming attacks. *SIAM Journal on Control and Optimization*, 54(6):3084–3105, 2016.
- [13] G. Befekadu, V. Gupta, and P. Antsaklis. Risk-sensitive control under markov modulated denial-of-service (DoS) attack strategies. *IEEE Transactions on Automatic Control*, 60(12):3299–3304, 2015.
- [14] A. Gupta, C. Langbort, and T. Başar. Dynamic games with asymmetric information and resource constrained players with applications to security of cyberphysical systems. *IEEE Transactions on Control of Network Systems*, 4(1):71–81, 2016.
- [15] W. Xu, G. Hu, D. Ho, and Z. Feng. Distributed secure cooperative control under Denial-of-Service attacks from multiple adversaries. *IEEE Transactions on Cybernetics*, 50(8):3458–3467, 2019.
- [16] A. Amini, A. Asif, and A. Mohammadi. Rq-cease: A resilient quantized collaborative event-triggered average-consensus sampled-data framework under denial of service attack. *IEEE Transactions on Systems, Man, and Cybernetics: Systems*, 51(11):7027–7039, 2020.
- [17] Z. Biron, S. Dey, and P. Pisu. Real-time detection and estimation of denial of service attack in connected vehicle systems. *IEEE Transactions on Intelligent Transportation Systems*, 19(12):3893–3902, 2018.
- [18] C. Deng, D. Zhang, and G. Feng. Resilient cooperative output regulation for mass with unknown switching exosystem dynamics under DoS attacks. *Automatica*, 139:110172, 2022.
- [19] H. Ishii and B. Francis. *Limited Data Rate in Control Systems with Networks*. Lecture Notes in Control and Information Sciences, vol. 275, Springer, 2002.
- [20] A. Kashyap, T. Başar, and R. Srikant. Quantized consensus. *Automatica*, 43(7):1192–1203, 2007.
- [21] S. Dibaji, H. Ishii, and R. Tempo. Resilient randomized quantized consensus. *IEEE Transactions on Automatic Control*, 63(8):2508–2522, 2017.
- [22] A. Rikos, C. Hadjicostis, and K. H. Johansson. Non-oscillating quantized average consensus over dynamic directed topologies. *Automatica*, 146:110621, 2022.
- [23] E. Xargay, R. Choe, N. Hovakimyan, and I. Kaminer. Multi-leader coordination algorithm for networks with switching topology and quantized information. *Automatica*, 50(3):841–851, 2014.
- [24] S. Kar and J. Moura. Distributed consensus algorithms in sensor networks: Quantized data and random link failures. *IEEE Transactions on Signal Processing*, 58(3):1383–1400, 2009.
- [25] W. Liu, J. Sun, G. Wang, F. Bullo, and J. Chen. Resilient control under quantization and Denial-of-Service: Co-designing a deadbeat controller and transmission protocol. *IEEE Transactions on Automatic Control*, 67(8):3879–3891, 2022.
- [26] K. You and L. Xie. Network topology and communication data rate for consensusability of discrete-time multi-agent systems. *IEEE Transactions on Automatic Control*, 56(10):2262–2275, 2011.
- [27] S. Feng and H. Ishii. Dynamic quantized consensus of general linear multiagent systems under Denial-of-Service attacks. *IEEE Transactions on Control of Network Systems*, 9(2):562–574, 2022.
- [28] S. Feng, M. Ran, H. Ishii, and S. Xu. Dynamic quantized consensus under DoS attacks: Towards a tight zooming-out factor. *IEEE Transactions on Control of Network Systems*, DOI: 10.1109/TCNS.2023.3281555, 2023.
- [29] M. Ran, S. Feng, J. Li, and L. Xie. Quantized consensus under data-rate constraints and DoS attacks: A zooming-in and holding approach. *IEEE Transactions on Automatic Control*, 68(9):5397–5412, 2023.
- [30] D. Li and T. Li. Cooperative output feedback tracking control of stochastic linear heterogeneous multi-agent systems. *IEEE Transactions on Automatic Control*, 68(1):47–62, 2023.
- [31] L. Ding, Q. Han, B. Ning, and D. Yue. Distributed resilient finite-time secondary control for heterogeneous battery energy storage systems under Denial-of-Service attacks. *IEEE Transactions on Industrial Informatics*, 16(7):4909–4919, 2019.
- [32] M. Ran and L. Xie. Practical output consensus of nonlinear heterogeneous multi-agent systems with limited data rate. *Automatica*, 129:109624, 2021.
- [33] S. Tatikonda and S. Mitter. Control under communication constraints. *IEEE Transactions on Automatic Control*, 49(7):1056–1068, 2004.
- [34] G. Nair and R. Evans. Stabilizability of stochastic linear systems with finite feedback data rates. *SIAM Journal on Control and Optimization*, 43(2):413–436, 2004.
- [35] M. Wakaiki, A. Cetinkaya, and H. Ishii. Stabilization of networked control systems under DoS attacks and output quantization. *IEEE Transactions on Automatic Control*, 65(8):3560–3575, 2019.
- [36] Y. Su and J. Huang. Cooperative output regulation of linear multi-agent systems. *IEEE Transactions on Automatic Control*, 57(4):1062–1066, 2011.
- [37] M. Guo and C. De Persis. Linear quadratic network games with dynamic players: Stabilization and output convergence to nash equilibrium. *Automatica*, 130:109711, 2021.
- [38] S. Battilotti, F. Cacace, C. Califano, and M. d’Angelo. Leader-following consensus with non-uniform and large communication delays. *IEEE Transactions on Control of Network Systems*, early access, 2023.
- [39] A. Shariati and M. Tavakoli. A descriptor approach to robust leader-following output consensus of uncertain multi-agent systems with delay. *IEEE Transactions on Automatic Control*, 62(10):5310–5317, 2016.
- [40] H. Moradian and S. Kia. A study on accelerating average consensus algorithms using delayed feedback. *IEEE Transactions on Control of Network Systems*, 10(1):157–168, 2023.